INTERNATIONAL JOURNAL FOR NUMERICAL METHODS IN FLUIDS
Int. J. Numer. Meth. Fluids 2006; **50**:973–985
Published online 17 October 2005 in Wiley InterScience (www.interscience.wiley.com). DOI: 10.1002/fld.1095

A short note on the entrainment and exit boundary conditions

P. Rajesh Kanna[‡,§] and Manab Kumar Das[*,†,¶]

Department of Mechanical Engineering, Indian Institute of Technology Guwahati, North Guwahati, Guwahati 781039, Assam, India

SUMMARY

An attempt is made to find out the suitable entrainment and exit boundary conditions in laminar flow situations. Streamfunction vorticity formulation of the Navier–Stokes equations are solved by ADI method. Two-dimensional laminar plane wall jet flow is used to test different forms of the boundary conditions. Results are compared with the experimental and similarity solution and the proper boundary condition is suggested. The Kind 1 boundary condition is recommended. It consists of zero first derivative condition for velocity variable and for streamfunction equation, mixed derivative at the entrainment and exit boundaries. Copyright © 2005 John Wiley & Sons, Ltd.

KEY WORDS: entrainment; streamfunction; boundary conditions; plane wall jet

1. INTRODUCTION

Entrainment occurs when a jet of fluid flows in an open domain. Flow over a flat plate, jet impingement on a plate, jet spread along a solid wall and jet emission into a quiescent domain are few examples where entrainment occurs. It has wide industrial applications like electronics cooling, turbine blade cooling, defroster system and high speed engine cooling, etc. While solving the problem numerically in streamfunction vorticity formulation, there are many ways to treat the boundary: few of them are Neumann boundary condition, Dirichlet boundary condition and close form analytical expression. Vynnycky *et al.* [1] have followed an analytical expressions for stream function (ψ) and vorticity (ω) for solving flow over a flat plate problem. They have considered the 'effective infinity' to treat the entrainment condition. Angirasa [2] has used Dirichlet boundary condition for velocity component at infinity for solving buoyant wall jet. He used the gradients of stream function taken to be equal to zero on the free sides. This physically implies that far away from the walls, the flow enters

*Correspondence to: Manab Kumar Das, Department of Mechanical Engineering, Indian Institute of Technology Guwahati, North Guwahati, Guwahati 781039, Assam, India.
†E-mail: manab@iitg.ernet.in
‡E-mail: rajeshk@iitg.ernet.in
§Research Scholar.
¶Associate Professor.

Received 1 May 2005
Revised 12 August 2005
Accepted 13 August 2005

and leaves the computational domain normal to the boundary. Al-Sanea [3, 4] has followed first derivative equal to zero as exit boundary condition for treating continuously moving plate problem. For entrainment velocity calculations its value depends upon the mass flow rate drawn outside the calculation domain by the viscous action of the moving plate. Han *et al.* [5] have investigated a discrete artificial boundary condition in stream function and vorticity formulation. They tested a few problems, viz. channel flow, flow over an obstacle, flow over backward facing step and flow over forward facing step problem and compared with Dirichlet and Neumann boundary conditions. Finally they concluded from the numerical results obtained that the boundary condition is very effective. Rao *et al.* [6] have used cross derivative for stream-function at entrainment and they have used potential flow, i.e. vorticity as zero value while solving mixed convection along flat plate. The present work is originated from the reviewer's comments of Kanna and Das [7] about the treatment of entrainment and exit boundary condition for an offset jet flow.

The present investigation is concerned about finding a suitable form to treat the entrainment and exit boundary condition. The study is carried out with an example problem of two-dimensional laminar incompressible plane wall jet flow. When a jet of fluid issues from a slit and spread along a wall, it forms a wall jet. It has inner region which behaves like a boundary layer flow over a flat plate and outer region behaves like a free shear layer [8]. The similarity profile has a point of inflexion. Glauert [9] has presented close form solution for plane wall jet of laminar as well as turbulent flow. Quintana *et al.* [10] have reported experimental results for laminar plane wall jet where surrounding is quiescent. Similar situation is considered for the present investigation of wall jet flow.

2. MATHEMATICAL FORMULATION

An incompressible two-dimensional laminar plane wall jet is considered. For the sake of simplicity, the jet is assumed to be isothermal and having the same density as the ambient fluid. Also, the velocity profile at the jet inlet is taken as parabolic. The schematic of the problem is shown in Figure 1 and the boundary conditions are shown in Figure 2. The boundary layer thickness δ is defined as the normal distance from the wall upto the distance where the velocity is half of local u maximum.

The governing equations for incompressible laminar flow are solved by stream function-vorticity formulation. The transient non-dimensional governing equations in the conservative form are

Stream function equation:

$$\nabla^2\psi = -\omega \tag{1}$$

Vorticity equation:

$$\frac{\partial\omega}{\partial t} + \frac{\partial(u\omega)}{\partial x} + \frac{\partial(v\omega)}{\partial y} = \frac{1}{Re}\nabla^2\omega \tag{2}$$

where ψ-stream function, $u = \frac{\partial\psi}{\partial y}$; $v = -\frac{\partial\psi}{\partial x}$ and $\omega = \frac{\partial v}{\partial x} - \frac{\partial u}{\partial y}$.

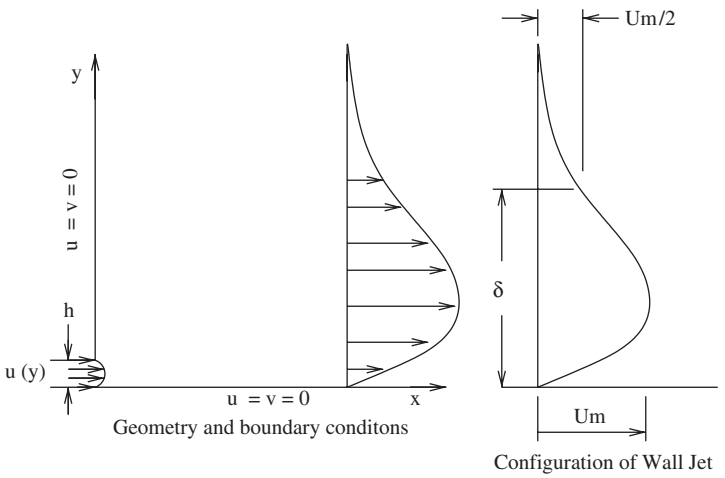

Figure 1. Schematic diagram and similarity profile of wall jet.

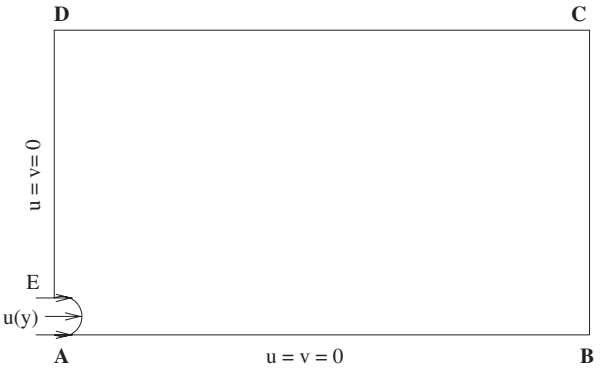

Figure 2. Boundary conditions in a plane wall jet problem.

The variables are scaled as

$$u = \frac{\bar{u}}{\bar{U}}; \quad v = \frac{\bar{v}}{\bar{U}}; \quad x = \frac{\bar{x}}{h}; \quad y = \frac{\bar{y}}{h}; \quad \omega = \frac{\bar{\omega}}{\bar{U}/h}; \quad t = \frac{\bar{t}}{h/\bar{U}}$$

with the overbar indicating a dimensional variable and $\bar{U}, h$ denoting the average jet velocity at nozzle exit and the jet width, respectively.

The boundary conditions needed for the numerical simulation have been prescribed. For plane wall jet with entrainment, the following dimensionless conditions have been enforced as shown in Figure 2. The inlet slot height is assumed as $h = 0.05$.

At the jet inlet, along AE (Figure 2)

$$u(y) = 120y - 2400y^2; \quad \omega(y) = 4800y - 120; \quad \psi(y) = 60y^2 - 800y^3 \tag{3a}$$

Along AB and ED due to no-slip condition

$$u = v = 0 \tag{3b}$$

Along DC

$$\frac{\partial u}{\partial y} = 0 \quad \text{or} \quad \frac{\partial v}{\partial y} = 0 \quad \text{or} \quad v = 0 \tag{3c}$$

At downstream boundary, the condition of zero first-derivative has been applied for velocity components. This condition implies that the flow has reached a developed condition. Thus, at (BC)

$$\frac{\partial u}{\partial x} = \frac{\partial v}{\partial x} = \frac{\partial \omega}{\partial x} = 0 \tag{3d}$$

Similar type of boundary conditions have been used by Al-Sanea [3, 4]. For comparison and validation with available experimental and numerical work, two cases namely, plane wall jet and plane sudden-expansion flow problems have been solved. In the second case, all the walls except the inlet and the outlet are solid. Thus there is no entrainment from the atmosphere and the boundary conditions are no-slip for these surfaces.

3. NUMERICAL PROCEDURE

The unsteady vorticity transport equation (2) in time is solved by alternate direction implicit scheme (ADI). Solution approaches steady-state asymptotically while the time reaches infinity. The computational domain considered here is clustered Cartesian grids. For unit length, the grid space at ith node is [11]

$$x_i = \left(\frac{i}{i_{\max}} - \frac{\kappa}{\vartheta} \sin\left(\frac{i\vartheta}{i_{\max}} \right) \right) \tag{4}$$

where ϑ is the angle and κ is the clustering parameter. $\vartheta = 2\pi$ stretches both end of the domain whereas $\vartheta = \pi$ clusters more grid points near one end of the domain. κ varies between 0 to 1. When it approaches 1, more points fall near the end.

The central differencing scheme is followed for both the convective as well as the diffusive terms [12]. It consists of two half time-steps. For details of the disctretization procedure, readers are referred to the article Kanna and Das [7].

The velocity components are updated by the following equations:

$$u = \frac{\partial \psi}{\partial y} = \frac{\psi_{i,j+1} - \psi_{i,j-1}}{\triangle y_j + \triangle y_{j-1}} \tag{5a}$$

$$v = -\frac{\partial \psi}{\partial x} = \frac{\psi_{i+1,j} - \psi_{i-1,j}}{\triangle x_i + \triangle x_{i-1}} \tag{5b}$$

The velocities are calculated at nth time level while advancing to the $(n+1)$th time level. Because of this approximation in the nonlinear terms, the second-order accuracy of the method is somewhat lost. However, something of the second-order accuracy of the linearized system is retained if the velocity field is slowly varying [12].

It is first-order accurate in time and second-order accurate in space $O(\Delta t, \Delta x^2, \Delta y^2)$, and is unconditionally stable. The streamfunction equation (1) is solved explicitly by five point Gauss–Seidel methods. Thom's vorticity condition has been used to obtain the wall vorticity as given below

$$\omega_w = -\frac{2(\psi_{w+1} - \psi_w)}{\Delta n^2} \tag{6}$$

where Δn is the grid space normal to the wall. It has been shown by Napolitano *et al.* [13] and Huang and Wetton [14] that convergence in the boundary vorticity is actually second-order for steady problems and for time-dependent problems when $t > 0$. Roache [12] has reported that for a Blausius boundary-layer profile, numerical test verifies that this first-order form is more accurate than second-order form.

At the bottom wall and the left side wall, constant stream lines are assumed based on inlet flow. At the outlet in the downstream direction, streamwise gradients are assumed to be zero. At the entrainment boundary, normal velocity gradient is zero [15].

The detailed boundary conditions are

Along ED (Figure 2):

$$\omega(y) = \frac{2(\psi_w - \psi_{w+1})}{\triangle x_1 * \triangle x_1}; \quad \psi = 0.05 \tag{7a}$$

Along AB:

$$\omega(x) = \frac{2(0 - \psi_{w+1})}{\triangle y_1 * \triangle y_1}; \quad \psi = 0 \tag{7b}$$

Entrainment boundary (DC) and exit boundary (BC) are tested by different form of boundary conditions namely Kind I, Kind II and Kind III.

Kind 1:

Along DC

$$\frac{\partial^2 \psi}{\partial x \partial y} = 0 \quad \left(\text{from } \frac{\partial v}{\partial y} = 0, \text{ Equation (3c)}\right) \tag{8a}$$

Discretizing Equation (8a) we get

$$\psi_{i,j} = \psi_{i-1,j} + \psi_{i,j-1} - \psi_{i-1,j-1} \tag{8b}$$

From the condition (Equation (3c))

$$\frac{\partial u}{\partial y} = 0, \quad u_{i,j} = u_{i,j-1} \tag{8c}$$

$$v_{i,j} = -\frac{(\psi_{i+1,j} - \psi_{i-1,j})}{\Delta x_i + \Delta x_{i-1}} \tag{8d}$$

$$\omega_{i,j} = \frac{(v_{i+1,j} - v_{i-1,j})}{(\Delta x_i + \Delta x_{i-1})} \tag{8e}$$

Along BC, ω, u, v, are evaluated based on zero gradient in the streamwise direction [12]. Backward difference scheme is followed for the first derivative at exit.

$$\frac{\partial^2 \psi}{\partial x \partial y} = 0 \quad \left(\text{from } \frac{\partial u}{\partial x} = 0, \text{ Equation (3d)}\right) \tag{8f}$$

Discretizing Equation (8f)

$$\psi_{i,j} = \psi_{i-1,j} + \psi_{i,j-1} - \psi_{i-1,j-1} \tag{8g}$$

$$\omega_{i,j} = \omega_{i-1,j} \tag{8h}$$

$$u_{i,j} = u_{i-1,j} \tag{8i}$$

$$v_{i,j} = v_{i-1,j} \tag{8j}$$

Kind 2:
Along DC
ψ, u, v and ω are evaluated as follows:

$$\frac{\partial^2 \psi}{\partial x \partial y} = 0 \quad \left(\text{from } \frac{\partial v}{\partial y} = 0, \text{ Equation (3c)}\right) \tag{9a}$$

Discretizing Equation (9a), we get

$$\psi_{i,j} = \psi_{i-1,j} + \psi_{i,j-1} - \psi_{i-1,j-1} \tag{9b}$$

$$u_{i,j} = u_{i,j-1} \quad \left(\text{from } \frac{\partial u}{\partial y} = 0, \text{ Equation (3c)}\right) \tag{9c}$$

$$v_{i,j} = -\frac{\partial \psi}{\partial x} = -\frac{(\psi_{i+1,j} - \psi_{i-1,j})}{\Delta x_i + \Delta x_{i-1}} \tag{9d}$$

$$\omega_{i,j} = \frac{(v_{i+1,j} - v_{i-1,j})}{(\Delta x_i + \Delta x_{i-1})} \tag{9e}$$

Along BC, ω, u, v, are evaluated based on streamwise direction first gradient is zero [12]. Backward difference scheme is followed for the first derivative at exit.

$$\frac{\partial^2 \psi}{\partial x^2} = 0 \quad \left(\text{from } \frac{\partial v}{\partial x} = 0, \text{ Equation (3d)}\right) \tag{9f}$$

Discretizing Equation (9f)

$$\psi_{i,j} = 2\psi_{i-1,j} - \psi_{i-2,j} \tag{9g}$$

$$\omega_{i,j} = \omega_{i-1,j} \tag{9h}$$

$$u_{i,j} = u_{i-1,j} \tag{9i}$$

$$v_{i,j} = v_{i-1,j} \tag{9j}$$

Equation (9f) is suggested by Roache [12] based on $\partial v/\partial x = 0$.

Kind 3:

Along DC

$$\frac{\partial u}{\partial y} = 0 \tag{10a}$$

$$u_{i,j} = u_{i,j-1} \tag{10b}$$

$$v_{i,j} = 0 \tag{10c}$$

from Equation (10c)

$$\psi_{i,j} = \psi_{i-1,j} \tag{10d}$$

$$\omega_{i,j} = \frac{(v_{i+1,j} - v_{i-1,j})}{(\Delta x_i + \Delta x_{i-1})} \tag{10e}$$

Along BC, ω, u and v are evaluated by Equations (8h)–(8j). ψ is evaluated by (9f) and (9g).

Along DC, Kind 1 and Kind 2 boundary expressions are common for ω, ψ, u and v. Kind 3 is different for v (Equation (10c)) and thus ψ expression is also different from Kind 1 and Kind 2. Along BC for ω, u, v Kind 1 is followed which is first-order accurate discretization based on first derivative equal to zero. Roache [12] suggested that first-order accurate terms are giving better results than second-order accurate approximation for the situations considered here. For ψ second-order accurate approximation is followed based on Equation (3d) ($\frac{\partial u}{\partial x} = 0$). In case of Kind 2, ψ is calculated based on Equation (3d) ($\frac{\partial v}{\partial x} = 0$). For ω, u and v, Kind 2 is identical with Kind 1. In case of Kind 3 along BC, ω, u and v are evaluated by Equations (8h)–(8j). Evaluation of ψ is performed by (9f) and (9g). These combinations of three boundary conditions for entrainment and exit situations are tested.

The maximum vorticity error behaviour is complicated as explained by Roache [12]. While marching in time for the solution, it has been observed that the maximum vorticity error gradually decreases. It then increases drastically and finally decreases asymptotically leading to steady-state solution. The convergence criteria is to be set in such a way that it should not terminate at false stage. At steady state, the error reaches the asymptotic behaviour. Here it is set as sum of vorticity error (Equation (11)) reduced to either the convergence criteria ε or elapsed large total time

$$\sum_{i,j=1}^{i_{\max}, j_{\max}} |(\omega_{i,j}^{t+\triangle t} - \omega_{i,j}^{t})| < \varepsilon \tag{11}$$

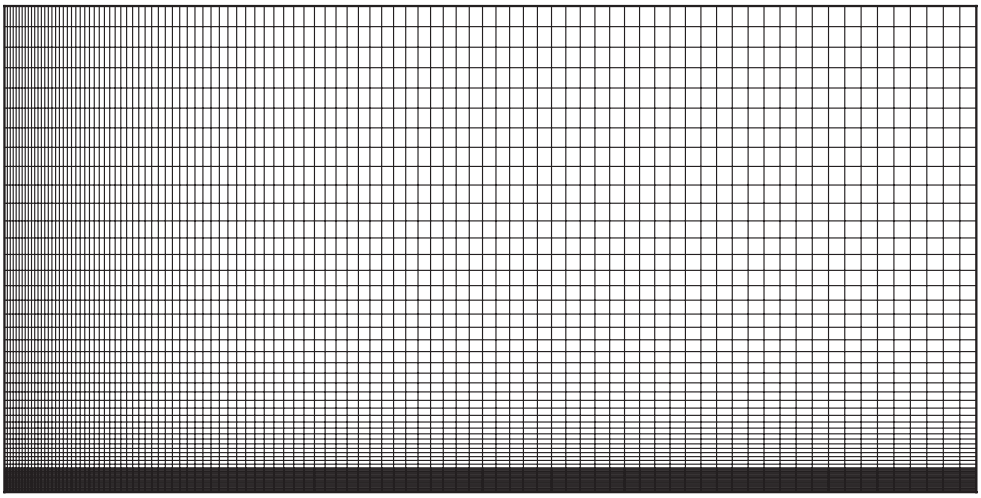

Figure 3. Grids for the computation (101×77, $\kappa = 0.7$).

4. VALIDATION OF THE CODE

To validate the developed code, the two-dimensional lid-driven square-cavity flow problem [16] is solved. Lid driven cavity flow is one of the benchmark problem which is having many flow physics like flow separation, boundary layer formation, etc. The agreement is good enough at high Reynolds number cases for capturing the vortices. The backward-facing flow problem is standard benchmark problem to test an inflow and outflow boundary conditions. Results are compared with References [17, 18] and excellent agreement is found among them [19]. Laminar offset jet flow is having flow separation, reattachment, development of flow in downstream direction and entrainment. The detailed results of the entrainment flow problem has been presented elsewhere [7, 20].

5. GRID INDEPENDENT STUDY

The domain has been chosen as $30 \times h$ in streamwise direction and $20 \times h$ in normal direction. Systematic grid refinement study is carried with 39×31, 51×41, 61×61, 71×61, 81×81 and 101×101. Grid refinement level 5 is used for the entire computations. The grids are clustered in streamwise direction whereas in normal direction up to $3 \times h$ height, grids are arranged uniformly and above this region, they are clustered. Typical grids are shown in Figure 3. The detail of the grid independent study is presented in Reference [21].

6. RESULTS AND DISCUSSION

Two-dimensional laminar incompressible plane wall jet flow is solved using different entrainment and exit boundary conditions. The steady state results are presented for $Re = 300$ case

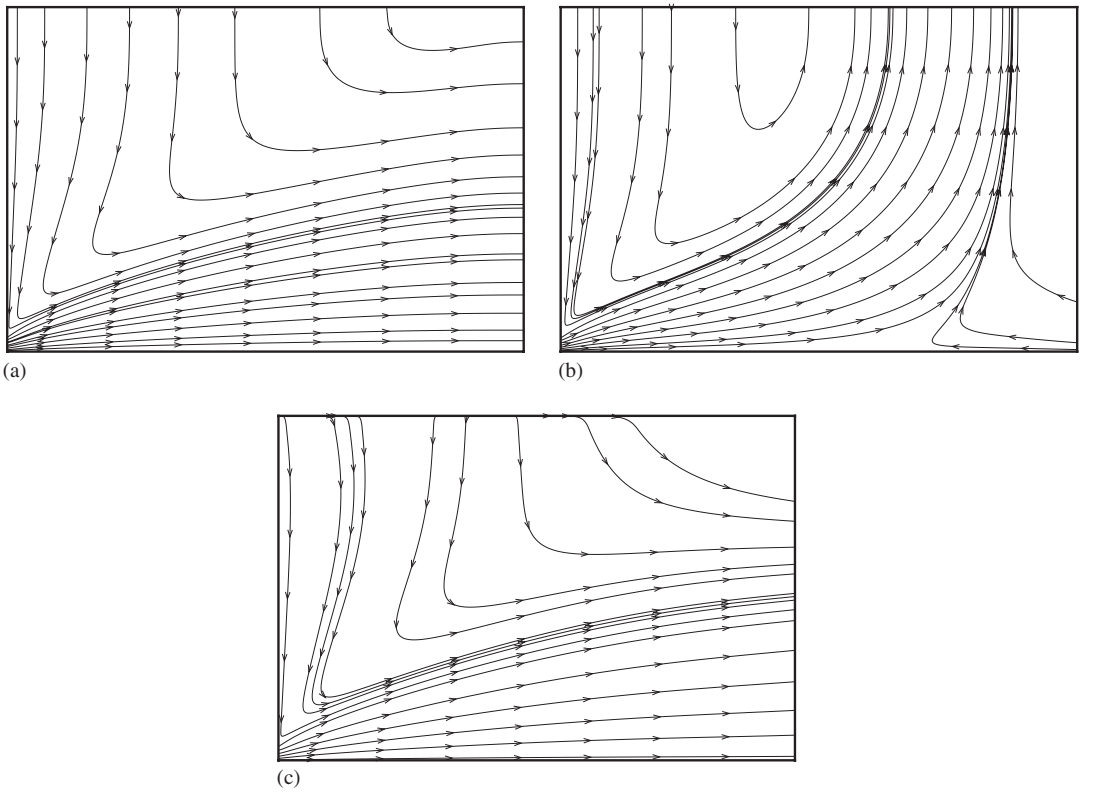

Figure 4. Stream trace plot for different boundary condition: $Re = 300$: (a) Kind 1; (b) Kind 2; and (c) Kind 3.

and the results are compared with the similarity solution of Reference [9] and the experimental results of Reference [10]. The stream function value can be derived from either u velocity or v velocity. The study is focused to find the suitable way to simulate the entrainment. Three different combination of boundary conditions are tested namely Kind 1, Kind 2 and Kind 3. The detailed velocity contours, stream line contours and similarity solutions are presented for these three boundary conditions.

The stream trace plot for different boundary conditions are shown in Figure 4. The stream trace consists of two regions: main flow and entrainment. For Kind 1 (Figure 4(a)) the main flow expands in the downstream direction. Entrainment occurs from the ambient which shears with main flow and is carried away in the downstream direction. For Kind 2 (Figure 4(b)), main flow exits through the entrainment surface CD instead of leaving from the exit region BC which is unrealistic. In case of Kind 3 (Figure 4(c)), the main flow exits through the downstream outflow passage BC and the stream trace near the top right corner is inclined to the downstream direction. The horizontal velocity (u) and normal direction velocity (v) components for the different boundary conditions considered here are presented in Figure 5. It is noticed that positive region and negative region are present in the u velocity contour for Kind 1 (Figure 5(a)). The entire main flow is having positive u value and near the left wall

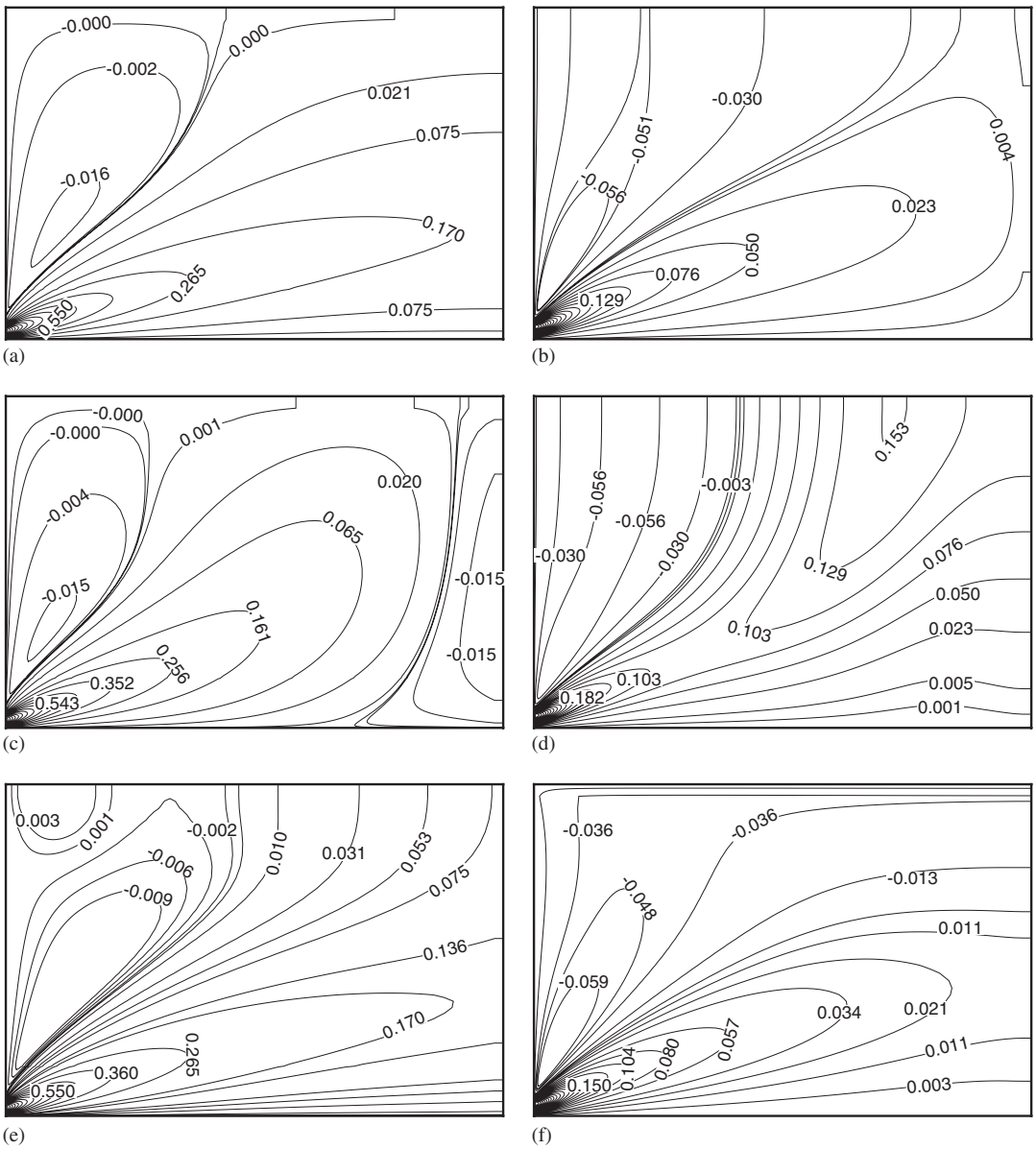

Figure 5. Velocity contour: $Re = 300$: (a) u velocity contour: Kind 1; (b) v velocity contour: Kind 1; (c) u velocity contour: Kind 2; (d) v velocity contour: Kind 2; (e) u velocity contour: Kind 3; and (f) v velocity contour: Kind 3.

negative u contours are present. Due to the pressure difference, flow occurs towards the entry of the jet. It is observed that near the boundary DC, u is approaching zero value. Figure 5(b) shows the v velocity contour for Kind 1 boundary condition. It is noticed that positive v value

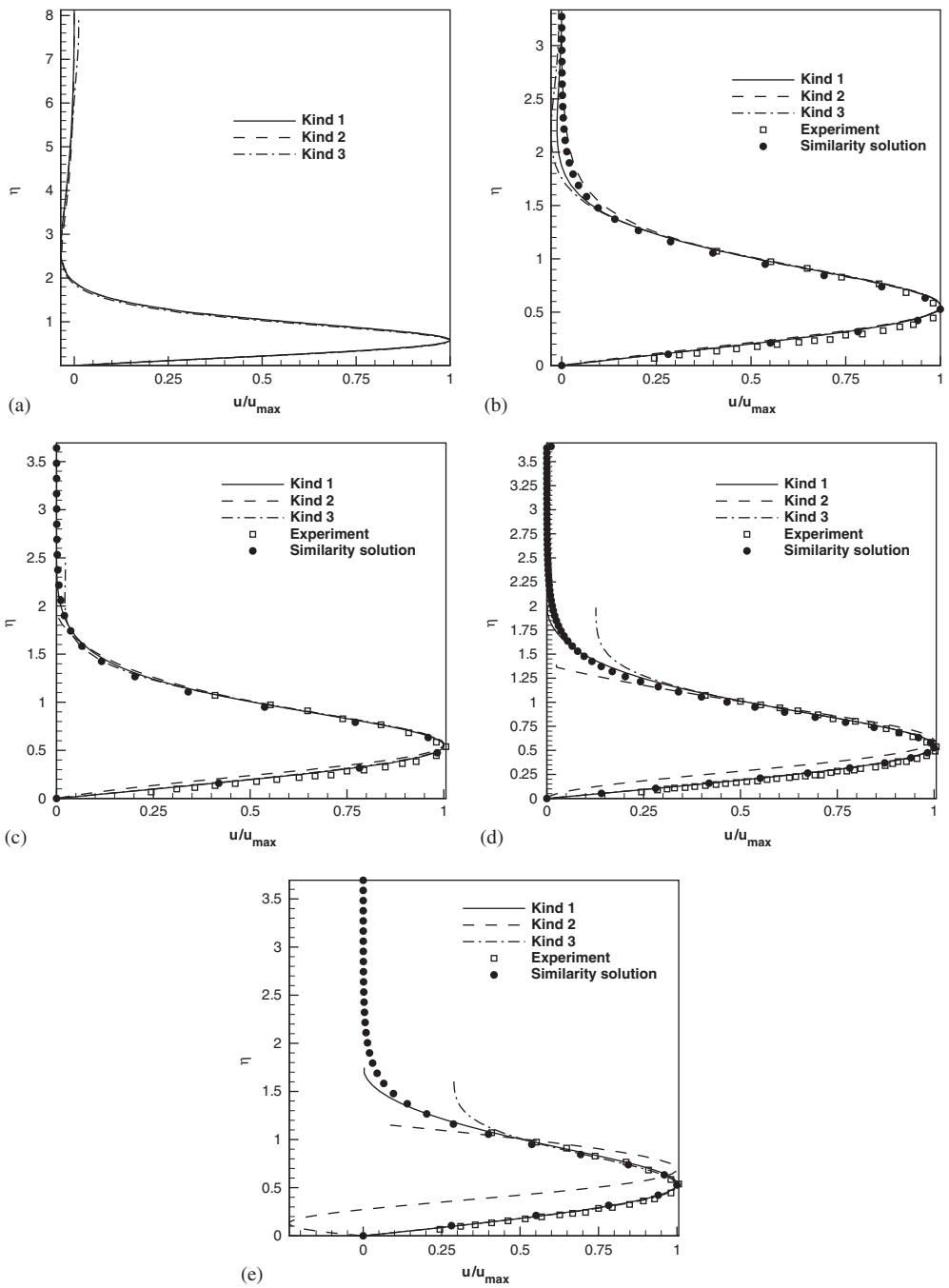

Figure 6. Similarity profile from different downstream location: $Re = 300$, experiment results by Quintana *et al.* [10]: (a) $x = 3h$; (b) $x = 10h$; (c) $x = 15h$; (d) $x = 20h$; and (e) $x = 25h$.

occurs at the main flow and negative values occur around entrainment. By the magnitude of the velocity near the entrainment boundary DC and exit boundary BC, it is observed that v is higher than u near the DC and u is higher than v near BC. For Kind 1 case, the streamfunction is evaluated based on these equations: along DC ψ is evaluated from $\partial v/\partial y = 0$ and along BC it is evaluated from $\partial u/\partial x = 0$. The u velocity contour and v velocity contour are presented for Kind 2 in Figures 5(c) and 5(d). Negative u velocity value is observed near the exit and positive v velocity is observed at the entrainment boundary. The u velocity contour is presented in Figure 5(e) for Kind 3. The main flow and entrainment along DC are simulated well by Kind 3 when compared with Kind 2. However, near the corner D positive u velocity is present. Close to a constant value is obtained for v velocity near DC which is parallel to the top entrainment surface (Figure 5(f)).

The boundary layer thickness (δ) is defined (Figure 1) as the normal distance where velocity is equal to $u_m/2$ and similarity variable (η) is defined as y/δ. Similarity profile at different down-stream location is shown in Figure 6. At $x = 3h$, the three boundary conditions are yielding the same velocity profile results (Figure 6(a)). The profile is having a small negative region at the shear layer of main flow with entrainment. Further downstream direction at $x = 10h$, the jet is expanded in the normal direction (Figure 6(b)). Results are compared with the similarity solution [22] and experimental results of Quintana *et al.* [10]. It is noticed that for Kind 1 and Kind 2, the velocity profile is having good agreement with them whereas for Kind 3, it is having good agreement with them upto certain distance in the outer region. Far away in the normal direction, it starts to deviate in the negative direction from the benchmark results. Figure 6(c) shows the similarity velocity profile at $x = 15h$ location. For Kind 1 and Kind 2, the velocity profiles are having good agreement with available results. In case of Kind 3 the velocity profile slightly deviates in the entrainment region. At $x = 20h$, the velocity profile Kind 1 is still having better agreement with standard benchmark results (Figure 6(d)) whereas for Kind 2 and Kind 3, the velocity profiles differ significantly from them. The similarity profile at $x = 25h$ location is shown in Figure 6(e). Kind 1 boundary condition has captured the wall jet similarity profile. Kind 2 has led to a reverse flow near the solid wall and u_m location is shifted in the normal direction compared to the benchmark similarity solution. For Kind 3, the velocity profile is having agreement with benchmark results upto part of the outer region and further in the normal direction it deviates and has constant u/u_m value which is higher than the benchmark value.

7. CONCLUSIONS

Numerical experiments are carried out to find the suitable entrainment and exit boundary conditions for laminar incompressible viscous flow situation. Stream function vorticity formulation of the governing equations are solved by ADI method. Two-dimensional laminar plane wall jet flow is considered for the study and the following conclusions are drawn. Near the entrainment boundary magnitude of normal direction velocity component is higher than the streamwise velocity component. Near the exit boundary, streamwise velocity component is higher than the normal direction velocity component. Streamfunction can be evaluated from either u or v velocity component. For boundary condition Kind 1, the velocity which has higher magnitude value is used. It shows excellent agreement with experimental as well as similarity solution. Kind 2 leads to erroneous results in the flow field. Reverse flow is observed

in the similarity profile. Authors feel that for entrainment like situation Kind 1 boundary condition is suitable to capture the flow physics. It consists of zero first derivative condition for velocity variable and for streamfunction equation, mixed derivative at the entrainment and exit boundaries.

ACKNOWLEDGEMENTS

The helpful comments of the reviewers are sincerely acknowledged by the authors.

REFERENCES

1. Vynnycky M, Kimura S, Kanev K, Pop I. Forced convection heat transfer from a flat plate: the conjugate problem. *International Journal of Heat and Mass Transfer* 1998; **41**:45–59.
2. Angirasa D. Interaction of low-velocity plane jets with buoyant convection adjacent to heated vertical surfaces. *Numerical Heat Transfer*, *Part A* 1999; **35**:67–84.
3. Al-Sanea SA. Convection regimes and heat transfer characteristics along a continuously moving heated vertical plate. *International Journal of Heat and Fluid Flow* 2003; **24**:888–901.
4. Al-Sanea SA. Mixed convection heat transfer along a continuously moving heated vertical plate with suction or injection. *International Journal of Heat and Mass Transfer* 2004; **47**:1445–1465.
5. Han H, Lu J, Bao W. A discrete artificial boundary condition for steady incompressible viscous flows in a no-slip channel using a fast iterative method. *Journal of Computational Physics* 1994; **114**:201–208.
6. Rao CG, Balaji C, Venkateshan SP. Conjugate mixed convection with surface radiation from a vertical plate with a discrete heat source. *Journal of Heat Transfer* 2001; **123**:698–702.
7. Kanna PR, Das MK. Numerical simulation of two-dimensional laminar incompressible offset jet flows. *International Journal for Numerical Methods in Fluids* 2005; **49**(4):439–464.
8. Bajura RA, Szewczyk AA. Experimental investigation of a laminar two-dimensional plane wall jet. *Physics of Fluids* 1970; **13**:1653–1664.
9. Glauert MB. The wall jet. *Journal of Fluid Mechanics* 1956; **1**(1):1–10.
10. Quintana DL, Amitay M, Ortega A, Wygnanski IJ. Heat transfer in the forced laminar wall jet. *Journal of Heat Transfer* 1997; **119**:451–459.
11. Kuyper RA, Van Der Meer ThH, Hoogendoorn CJ, Henkes RAWM. Numerical study of laminar and turbulent natural convection in an inclined square cavity. *International Journal of Heat and Mass Transfer* 1993; **36**(11):2899–2911.
12. Roache PJ. *Fundamentals of Computational Fluid Dynamics*, Chapter 3. Hermosa: U.S.A, 1998.
13. Napolitano M, Pascazio G, Quartapelle L. A review of vorticity conditions in the numerical solution of the $\zeta - \psi$ equations. *Computers and Fluids* 1999; **28**:139–185.
14. Huang H, Wetton BR. Discrete compatibility in finite difference methods for viscous incompressible fluid flow. *Journal of Computational Physics* 1996; **126**:468–478.
15. Kang SH, Greif R. Flow and heat transfer to a circular cylinder with a hot impinging air jet. *International Journal of Heat and Mass Transfer* 1992; **35**(9):2173–2183.
16. Ghia U, Ghia KN, Shin CT. High resolutions for incompressible flow using the Navier–Stokes equations and multigrid method. *Journal of Computational Physics* 1982; **48**:387–411.
17. Armaly BF, Durst F, Pereira JCF, Schonung B. Experimental and theoretical investigation of backward-facing step flow. *Journal of Fluid Mechanics* 1983; **127**:473–496.
18. Gartling DK. A test problem for outflow boundary conditions-flow over a backward-facing step. *International Journal for Numerical Methods in Fluids* 1990; **11**:953–967.
19. Kanna PR, Das MK. A note on the reattachment length for BFS problem. *International Journal for Numerical Methods in Fluids* 2005, in press.
20. Kanna PR, Das MK. Numerical simulation of two-dimensional laminar incompressible wall jet under backward-facing step flows. *Journal of Fluids Engineering* 2005, submitted.
21. Kanna PR, Das MK. Conjugate forced convection heat transfer from a flat plate by laminar plane wall jet flow. *International Journal of Heat and Mass Transfer* 2005; **48**:2896–2910.
22. Schlichting H, Gersten K. *Boundary Layer Theory* (8th edn). Springer: Berlin, 2000; 215–218.

